SUPPLEMETARY FIGURE LEGENDS

Supplementary Figure 1. (A) MTT assays demonstrate comparable proliferation rates in HCC cells, Hepa1-6 and Huh7 cells, under normoxic and hypoxic conditions. **(B)** Western blot of PGC-1α when Hepa1-6 cells were subjected to 24 hours of 21% O_2 (control), 5% O_2, and 1% O_2 (hypoxia). **(C)** Cancer cells labeled with MitoSOX subjected to flow cytometric analysis show increased intracellular ROS when PGC-1α is silenced.

Supplementary Figure 2. (A) Western blot analysis confirms decreased HMGB1 levels in HCC cells treated with HMGB1 siRNA. **(B)** Western blot of PGC-1α show no significant difference in expression between control and HMGB1-depleted cells in resting normoxic Hepa 1-6 cancer cells. **(C)** OCR data indicates significant decrease in basal respiration rate between HMGB1-depleted cells and control cells under normoxic conditions (21% O_2)**. (D)** Immunoflorescent images show increased intracellular ROS production (MitoSox staining) in HMGB1 deficient cells compared to controls. Nuclei (blue), Mitosox (green). **(E)** Western Blot of cleaved caspase 3 protein shows increased apoptosis in hypoxic Hepa1-6 and Huh7 cells treated with HMGB1 siRNA compared to control siRNA. **(F)** Invasion and migration transwell assays demonstrate significantly decreased migration and invasion if HMGB1-silenced HCC cells when subjected to hypoxia.

Supplementary Figure 3. (A) Flow Cytometry analysis of PGC-1α knockdown groups revealed 4-fold increase in apoptotic rates compare to control groups. **(B)** OCR data indicates significant changes in basal respiration rate between PGC-1 α siRNA treated cells and control cells during hypoxia. **(C)** Intracellular ATP levels in control and PGC-1α siRNA HCC cell lines in normoxia and at different time exposure to hypoxia. There is a significant decrease in ATP production

between control and PGC-1α siRNA HCC cells at each time point of hypoxia. Control cells regain their baseline normoxic ATP production capacity at 12 hours, *P<0.05, **P<0.01, ***P<0.001, ns: Not Significant.

Supplementary Figure 4. (A) Western blot of PGC-1α expression in nontumor tissues of control and Alb-HMGB1$^{-/-}$ mice. **(B and C)** Confocal microscopy showing no difference in the expression of PGC-1α and TOM20 in non-tumor tissues of control and Alb-HMGB1$^{-/-}$ mice.

Supplementary Figure 5. (A) Western blot analysis shows a decrease in expression of.electron transport chain proteins ND1 and COX3 in the tumors of Alb-HMGB1$^{-/-}$ compared to control mice **(B)** RT-PCR analysis reveals significant decrease in the expression of the various mitochondrial biogenesis associated proteins PGC-1α, TFAM and NRF1 in in Alb-HMGB1$^{-/-}$ tumors compared to control. **(C)** Confocal microscopy showing decrease in the expression of PGC-1α in tumor tissues of Alb-HMGB1$^{-/-}$ compared to control mice. **(D)** Western blot analysis shows an increase in caspase 3 activation in HMGB1-depleted tumors compared to control tumors.

Supplementary Figure 6. (A) Immunoprecipitation assay demonstrates that there is increased binding of HMGB1 and TLR9 during hypoxia in Hepa 1-6 cells compared to cells under normoxic condition or compared to control IgG. **(B and C)** Densitometry analysis of the western blot from three independent experiments. **P<0.001, *p<0.05, ns: not significant.

Supplementary Figure 7. (A) Confocal microscopy reveals increase PGC-1α expression in hypoxic Hep1-6 cells that overexpress HMGB1 (pHMGB1) compared to control. This increase in PGC-1α expression is not present if the cells were treated with a TLR9 antagonist. Also, there was a decrease in PGC-1α expression in hypoxic HMGB-1 deficient Hep1-6 cells, this was reversed when the cells were treated with a TLR9 agonist. **(B)** Western blot assay shows a

significant decrease in PGC-1α activation in TLR9 siRNA cells compared to cells treated with control siRNA during hypoxia.

SUPPLEMENTARY MATERIALS AND METHODS

Cell culture and Reagents

Hep1-6 and Huh7 cells were grown in Dulbecco's modified Eagle's medium (DMEM) containing 10% fetal bovine serum (FBS), 100 U/ml penicillin G, and 100μg/ml streptomycin, 15mmol/L HEPES, 200mmol/L L-Glutamine, and incubated at 37^{o}C in a humidified incubator containing 5% CO_2. The reagents and antibodies used for Western Blots were as follows: anti-p38/p-p38 (Cell Signaling); anti-actin (Sigma); anti HIF-1-alpha (Abcam); anti-PGC1 alpha (Abcam); anti-Phospho-PGC1α (RnD systems); anti-COX IV (Cell Signaling) anti-NRF1 (Cell Signaling); anti-mtTFA (Abcam); anti-HMGB1 (Abcam); anti-cleaved caspase 3 (Cell Signaling). TLR9 agonist (ODN 1668-2006) and antagonist (ODN 2088-TTAGGG) were purchased from InvivoGen.

Establishment of stable HMGB1 expressing Hep1-6 cells

Plasmids were transfected into cells with Lipofectin 2000. After 24 hours, transfected cells were spread onto 100-mm culture dish at 1:100 dilutions. Selection for stable transfection, cells were cultured in DMEM with 600μg/ml G418 (Sigma-Aldrich) for 4 weeks. Clones with G418 resistance were selected and expanded.

Immunoblotting

Western blot assays were performed using whole cell lysates from either liver tissue (tumor or non-tumor) or cell lines. Membranes were incubated overnight using the above mentioned antibodies.

Recombinant rhHMGB1

The full length cDNA for human HMGB1 was subcloned in-frame to the secretion signal of a modified YEpFLAG (Sigma). Modified plasmid contains a 6x His tag in place of the original FLAG tag. This vector was then transformed into the protease deficient yeast strain (BJ3505). The transformed yeast were grown at 30 o C for 3 days on a rotary shaker in 500 ml of Expression media (1% glucose, 3% glycerol, 1% yeast extract, 2% peptone, 100mM potassium phosphate, pH 6.4). The culture was chilled at 4oC and centrifuged and sufficient ammonium sulfate was added slowly to obtain a concentration of 80% After purification, the protein was dialyzed with 25mM Tris, 150 mM KCl pH 8.0 (1).

Quantitative real-time PCR

Total RNA was extracted from the cell using the RNeasy Mini Kit (Qiagen) according to the manufacturer's instruction. mRNA for the cytokines of interest and β-actin were quantified in duplicate by SYBR Green two-step, real-time reverse transcription polymerase chain reaction (RT-PCR). After removal of potentially contaminating DNA with DNAse I (Life Technologies), 2 μg of total RNA from each sample was used for Clontech cDNA synthesis kit (Clontech) to generate first-strand cDNA. PCR reaction mixture was prepared using SYBR Green PCR Master Mix (PE Applied Biosystems). Thermal cycling conditions were 10 min at 95°C followed by 40 cycles of 95°C for 15 s and 60°C for 1 min on an ABI PRISM 7000 Sequence Detection System (PE Applied Biosystems). Each gene expression was normalized with β-actin mRNA content.

Cell migration and invasion assays

The migration and invasion assays were performed by using Transwell insert chambers (6.5 mm diameter, 8 mm pore size, Corning) as previously described (2).

Cell Proliferation Assays

Cell proliferation was assessed using an MTT assay. Cells (1×10^3 cells/well) were seeded on

96-well plates and treated according to experimental requirements. 10µl of MTT was added to each well and the cells were incubated at 37°C for 4 h. Then, 100µl dimethylsulfoxide was added to each well and mix thoroughly to dissolve the dark blue crystals overnight. The optical density (OD) was measured at 550 nm using a microplate reader (Bio-Rad Model 690, Richmond, CA, USA).

Detection of cellular apoptosis and ROS production using flow cytometry

Cellular apoptosis was measured by using FITC Annexin V Apoptosis Detection Kit I (BD Pharmingen). Cancer cells were washed with cold PBS and resuspended in 1X Binding Buffer at the concentration of 100K (1 x 10^5 Cells) per 100ul. Cells were stained with 5ul of FITC and PI, and then incubated for 15 minutes at 25^0C. Mitochondrial ROS was measured by using MitoSox (Invitrogen) staining at the concentration of 5uM for 15 minutes at 37^0C.

Primers for mitochondrial DNA measurement

The following primers were used: mouse COXI forward, 5'-GCCCCAGATATAGCATTCCC-3'; mouse COXI reverse, 5'GTTCATCCT GTTCCTGCTCC-3', Mouse β-actin forward, 5'-AGAGGGAAATCGTGCGTGAC-3'; mouse β-actin reverse 5'CAATAGTGATGACCTGGCCGT-3'.

Tumor Burden Analysis

Mice were sacrificed at six months and the livers were harvested in toto for analysis. Liver and mice weights and gross metastatic surface nodules were assessed. Intrahepatic tumor burden was assessed by calculating the percentage of hepatic tissue replaced by tumor i.e. the hepatic replacement area (HRA) (3). On H&E stained histological sections at 40x magnification, the tumor occupied area was quantitatively assessed by Image J (NIH). Results were presented as the mean of the percentage of tumor occupying area (mm^2) with respect to the entire area of one

capture (mm^2).

Immunoprecipitation (IP)

Following treatment, whole lysate protein diluted in IP buffer (50mM 4-(2-hydroxyethyl)-1-piperazine ethanesulfonic acid, 0.5% Nonidet P-40, 150mM NaCl, 10% glycerol, 1mM EDTA). Normal rabbit IgG was used as a negative control, Whole-cell lysates (400µg) were incubated with 1µg anti-HMGB1 antibodies and 20µl protein A/G-beads at 4^oC overnight. Samples were washed with PBS and subjected to Western Blot analysis.

Confocal microscopy

Liver tissue from mice was removed after perfusion with cold PBS and 2% paraformaldehyde. Tissue was fixed in 2%paraformaldehyde for an additional 2 h followed by cryopreservation as previously described (4). Liver sections (6µm) were permeabilized with 0.1% Triton X-100 for 20 min, followed by five washes with PBS+0.5% BSA (PBB). Sample sections were incubated in PBB for 1 h at room temperature (RT) with the following primary antibodies directed against the protein of interest, in the presence of 0.1% Triton X-100 to facilitate antibody access to the epitope: 4-hydroxy-2-nonenal (HNE) Michael adducts HNE antibody (1:200 Calbiochem); TOM20 (1:50 SantaCruz); Ki67 (1:100 Abcam); TUNEL (Roche) with Biotin-16-dUTP (Roche); PGC-1a (1:100 Abcam); NRF1 (1:100 Cell Signaling); mtTFA (1:100 Abcam); MitoTracker Red CMRos (400nM Invitrogen). The samples were rinsed in PBS (5 times) to remove unbound primary antibodies. Cells plated on coverslips were processed similarly to *in vivo* samples. Secondary antibodies: cy5-conjugated streptavidin antibody (1:1000 Jackson-ImmunoResearch); Alexa Fluor-conjugated Cy3 anti-rabbit antibody (1:1000 Invitrogen) were added in PBB for 1 h at RT. Where indicated in figure legend, Alexa Fluor-conjugated 647 phallodin (1:500 Invitrogen) w**as** added in PBB for 1 h at RT. Tissue sections were then washed twice in PBS (3

times) and the nuclei were stained with a 15 second incubation with 1 mg/ml Hoechst (Sigma-Aldrich). Finally, after a PBS rinse the sections were coverslipped using aquamount mounting media. For controls, sections were treated excluding the primary antibody ("primary delete"), and the samples were imaged with microscope settings to minimize sample autofluorescences using the primary delete processed sample. All slides were scanned under the same conditions for magnification, exposure time, lamp intensity and camera gain.

Imaging was performed using either a Nikon A1 confocal microscope for tissue as a large area scan or using Olympus Fluoview 1000 microscope for *in vitro* samples at (×20 with and without a 2 digital zoom; purchased with 1S10OD019973-01 awarded to Dr. Simon C. Watkins). Quantification was performed using NIS Elements software (Nikon). The final figures were imported as Tiff format and assembled in Adobe Photoshop.

Transmission electron microscopy

Cells were fixed in 2% glutaraldehyde in 0.1 M phosphate buffer (pH 7.4) for I h and then switched to PBS and processed for microscopy. After dehydration, thin sections were stained with uranyl acetate and lead citrate for observation under a JEM 1011CX electron microscope (Jeol, Peobody, MA, USA). Images were acquired from randomly selected pool of 10-15 fields under each condition.

References

1. Ngamkitidechakul, C., and Twining, S.S. 2002. Buffered non-fermenter system for lab-scale production of

secreted recombinant His-tagged proteins in Saccharomyces cerevisiae. *Biotechniques* 33:1296-1300.

2. Chen, M., Liu, Y., Varley, P., Chang, Y., He, X.X., Huang, H., Tang, D., Lotze, M.T., Lin, J., and Tsung, A. 2015. High-Mobility Group Box 1 Promotes Hepatocellular Carcinoma Progression through miR-21-Mediated Matrix Metalloproteinase Activity. *Cancer Res* 75:1645-1656.
3. te Velde, E.A., Vogten, J.M., Gebbink, M.F., van Gorp, J.M., Voest, E.E., and Borel Rinkes, I.H. 2002. Enhanced antitumour efficacy by combining conventional chemotherapy with angiostatin or endostatin in a liver metastasis model. *Br J Surg* 89:1302-1309.
4. Huang, H., Nace, G.W., McDonald, K.A., Tai, S., Klune, J.R., Rosborough, B.R., Ding, Q., Loughran, P., Zhu, X., Beer-Stolz, D., et al. 2014. Hepatocyte-specific high-mobility group box 1 deletion worsens the injury in liver ischemia/reperfusion: a role for intracellular high-mobility group box 1 in cellular protection. *Hepatology* 59:1984-1997.

Supplementary Figure 1

A

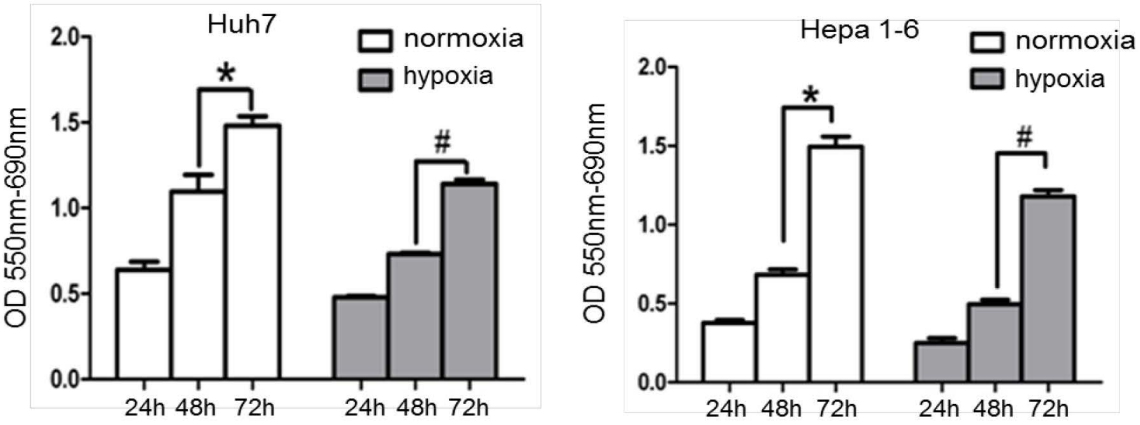

B

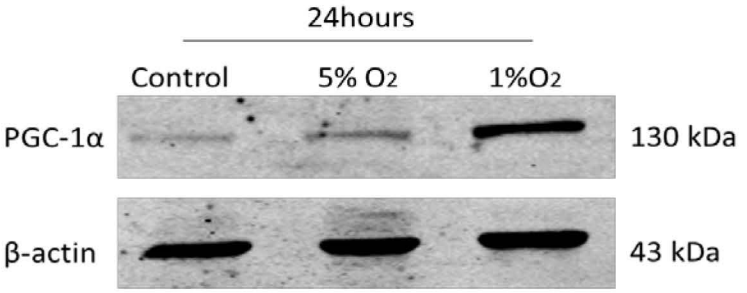

C

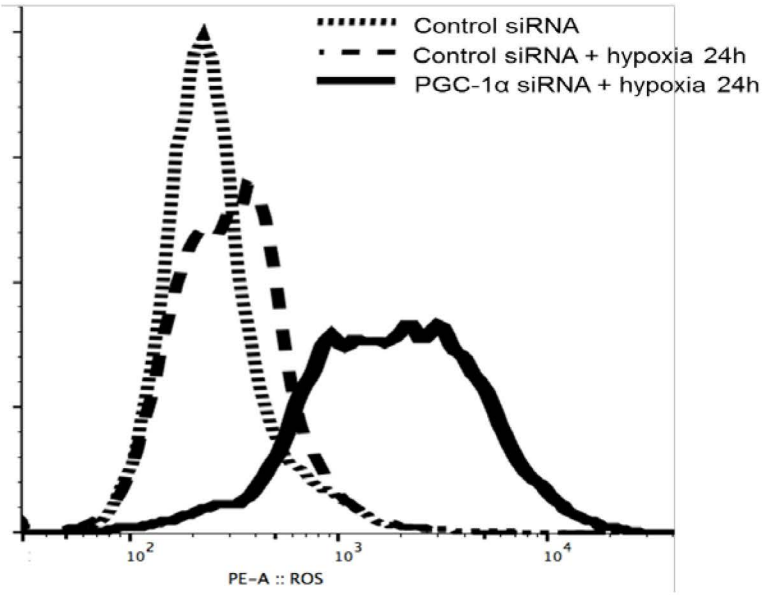

Supplementary Figure 2

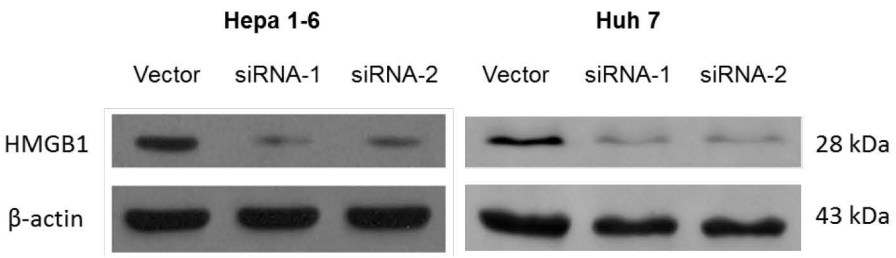

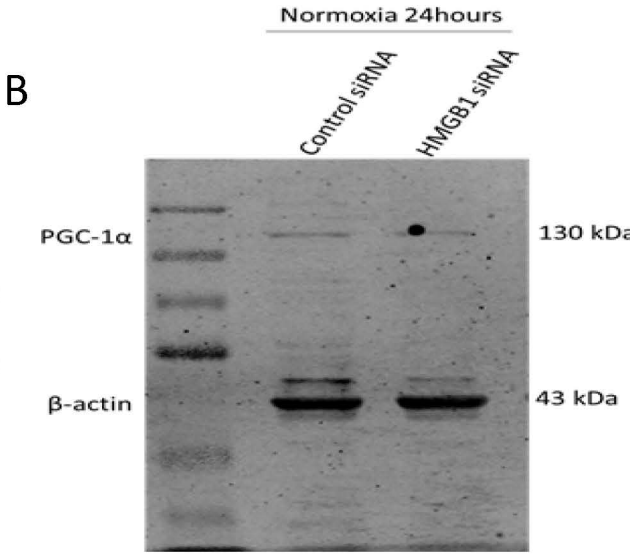

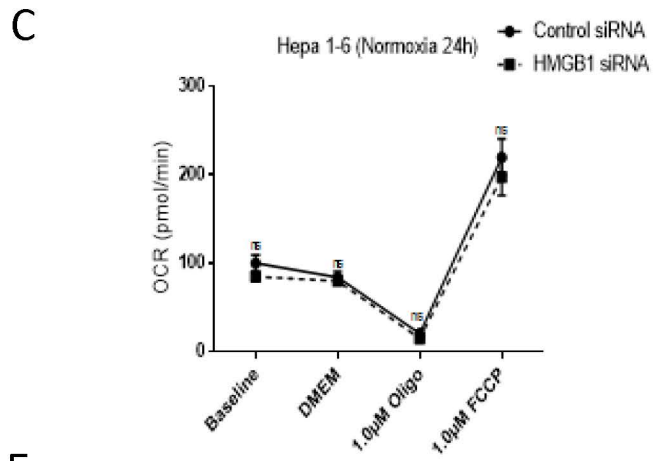

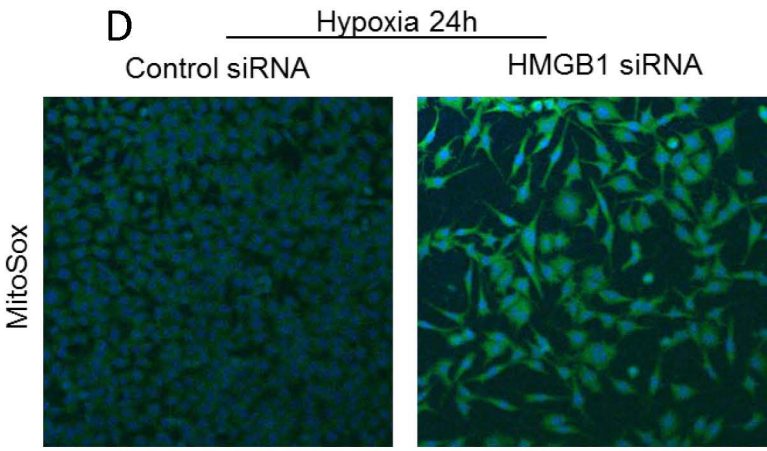

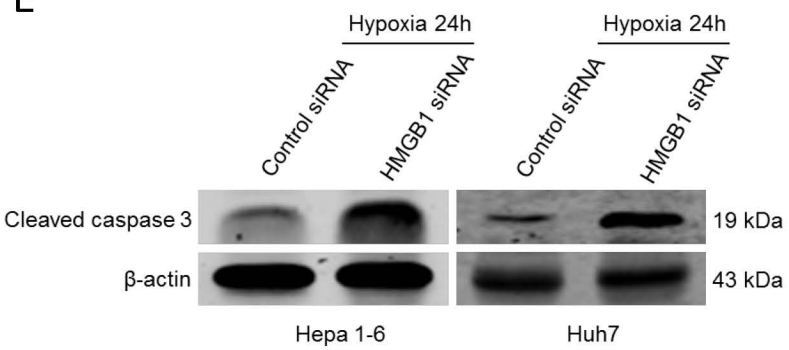

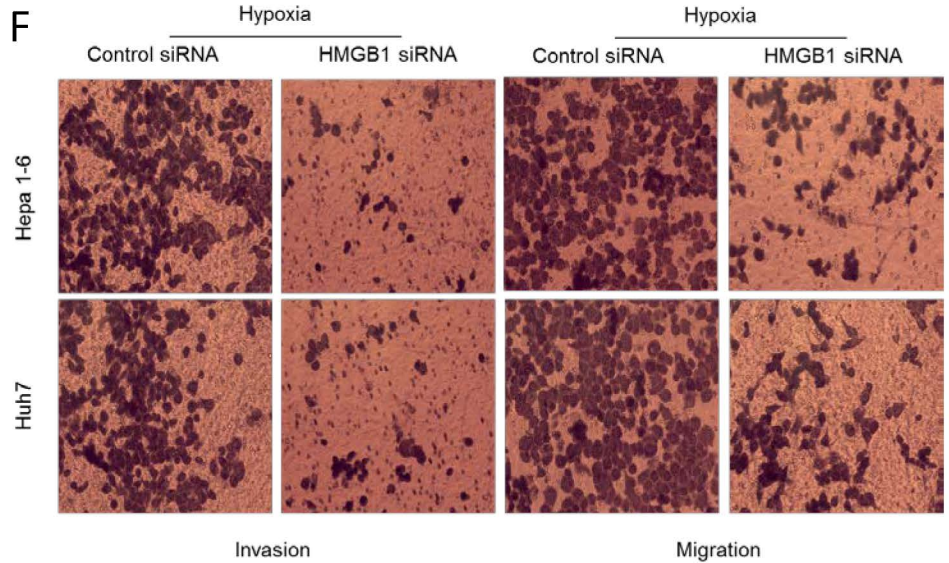

Supplementary Figure 3

A

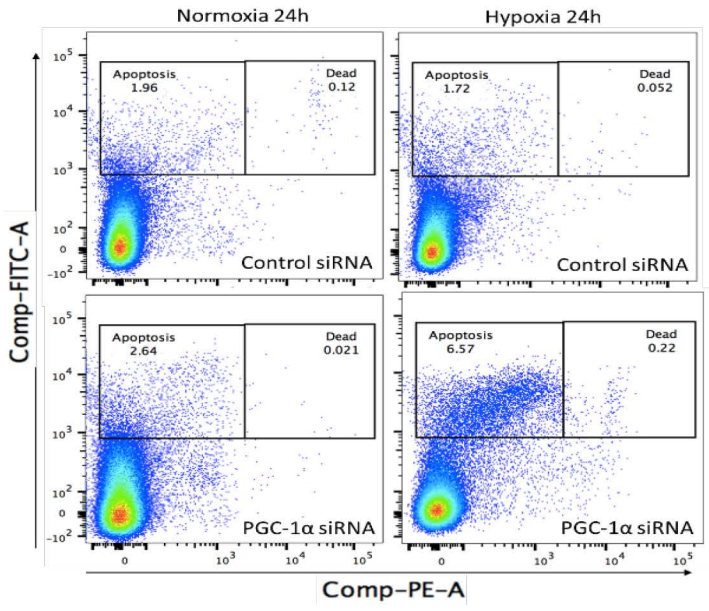

B

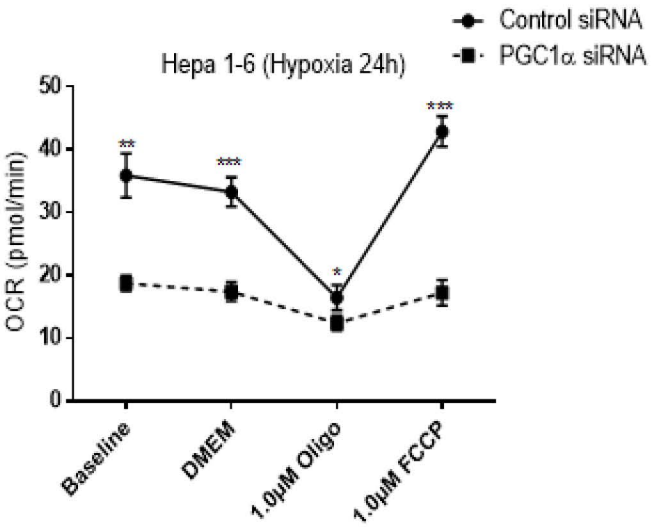

C

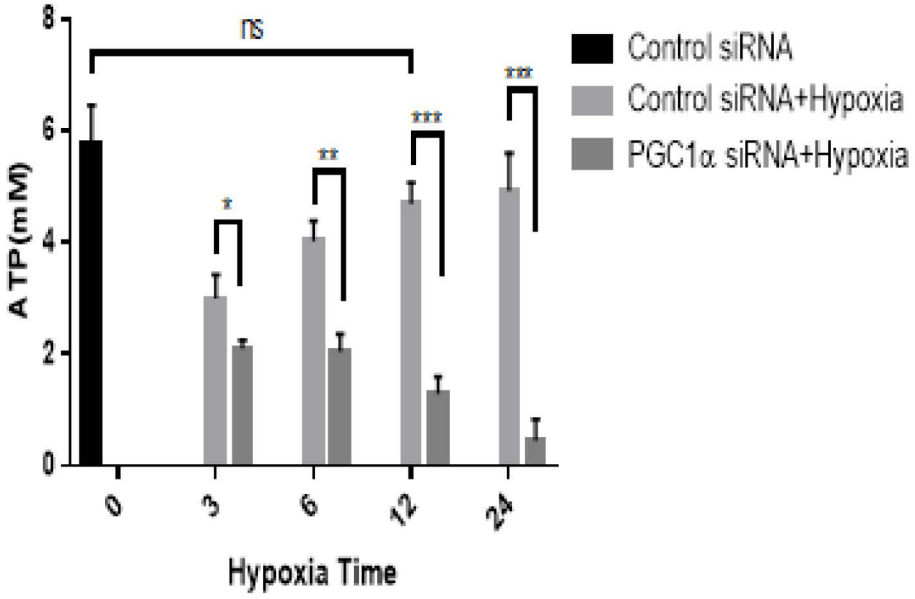

Supplementary Figure 4

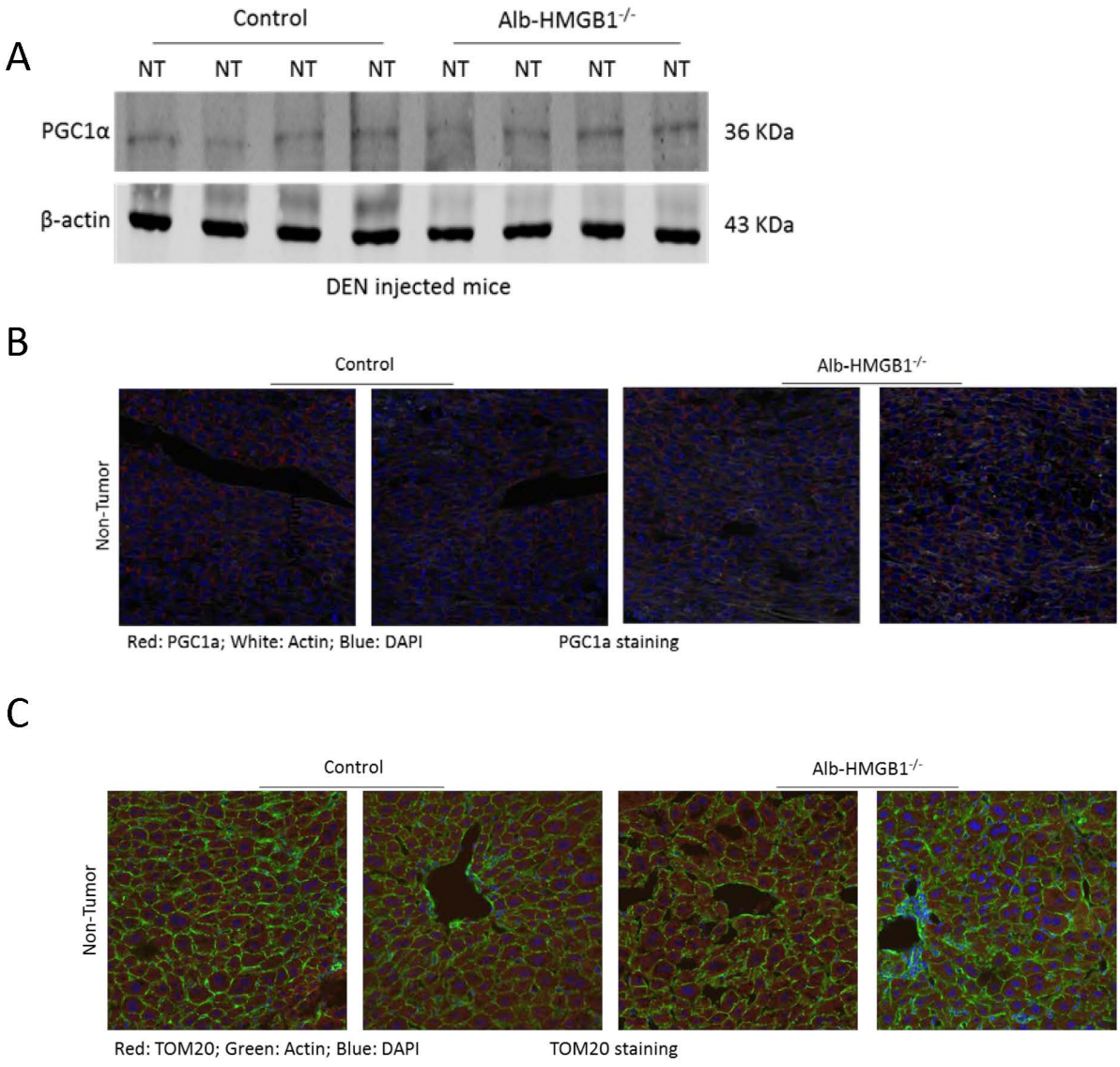

Supplementary Figure 5

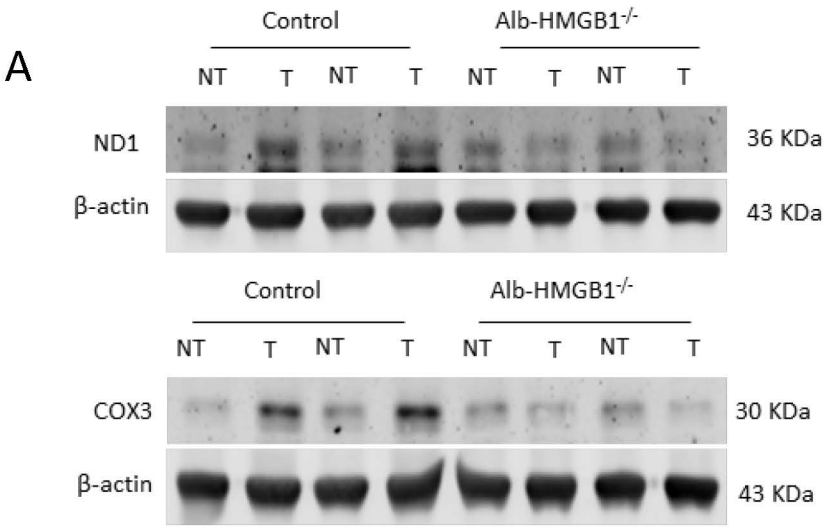

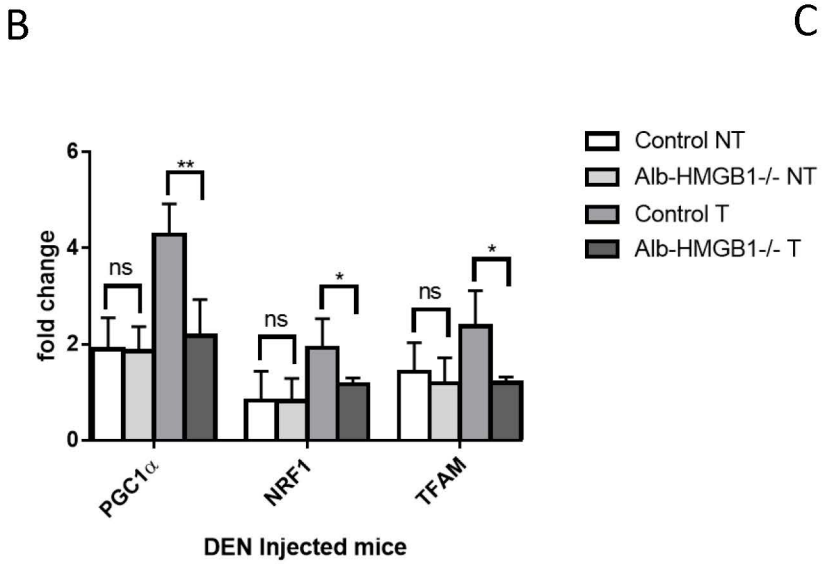

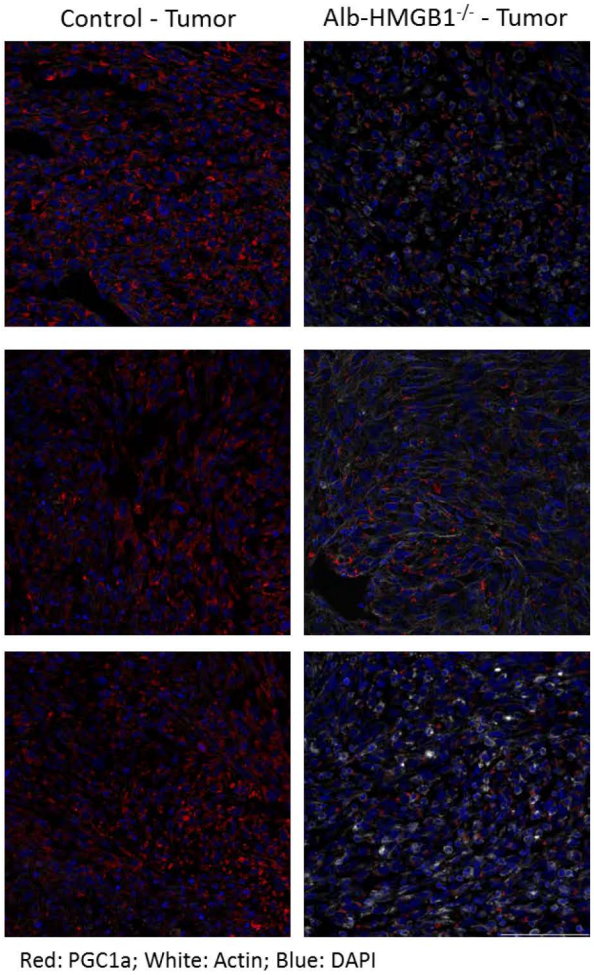

Red: PGC1a; White: Actin; Blue: DAPI

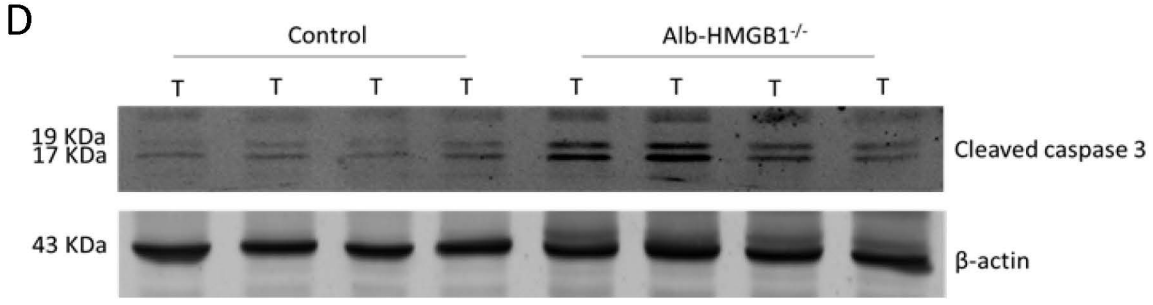

Supplementary Figure 6

A

B

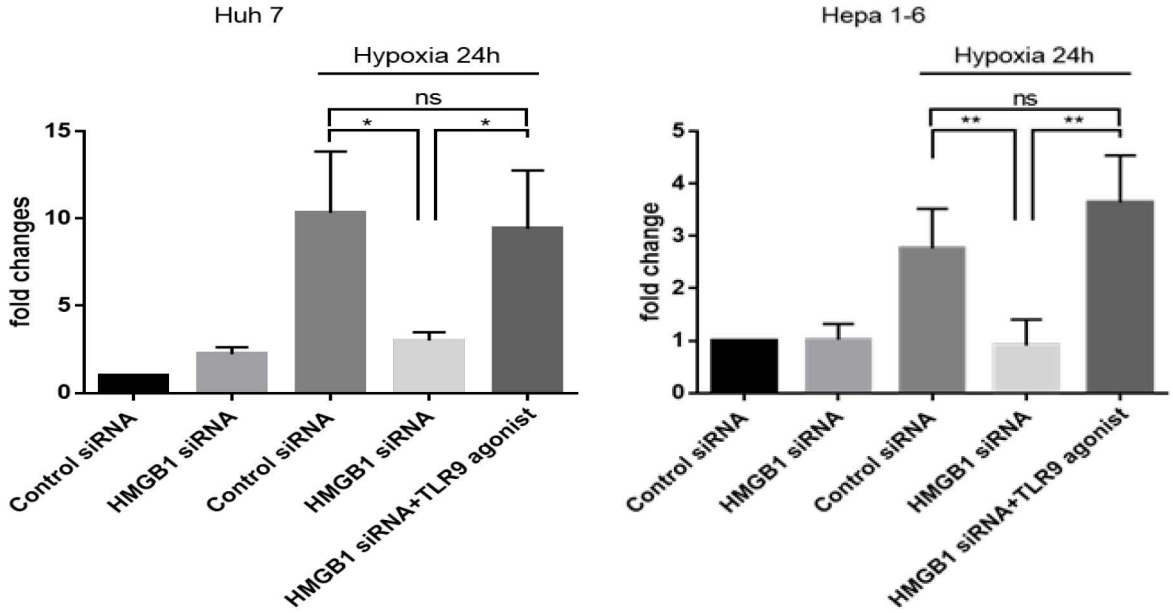

C

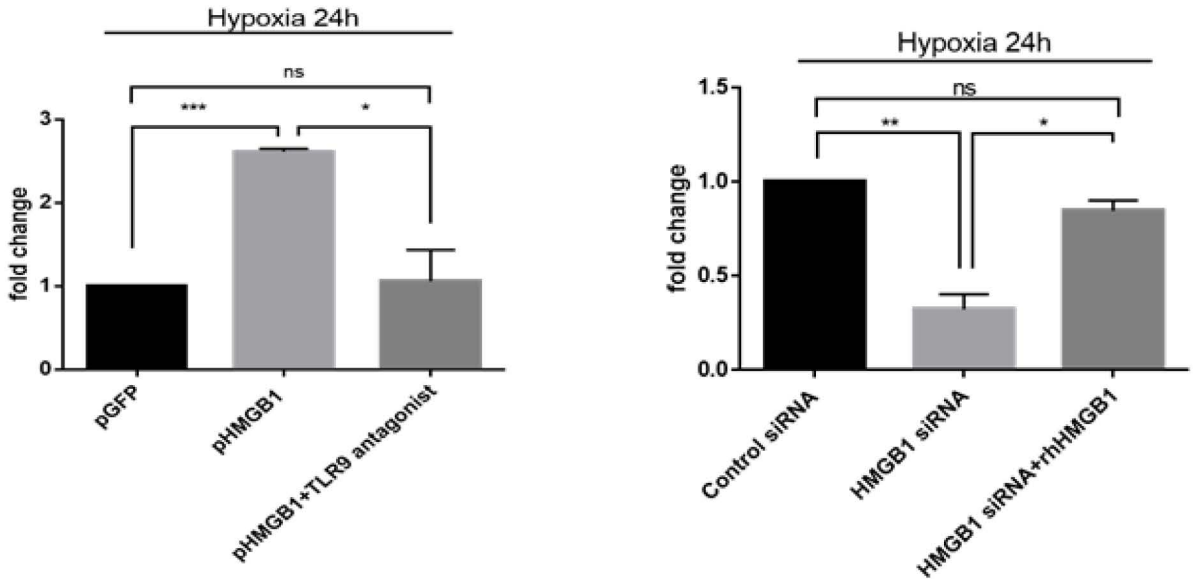

Supplementary Figure 7

A

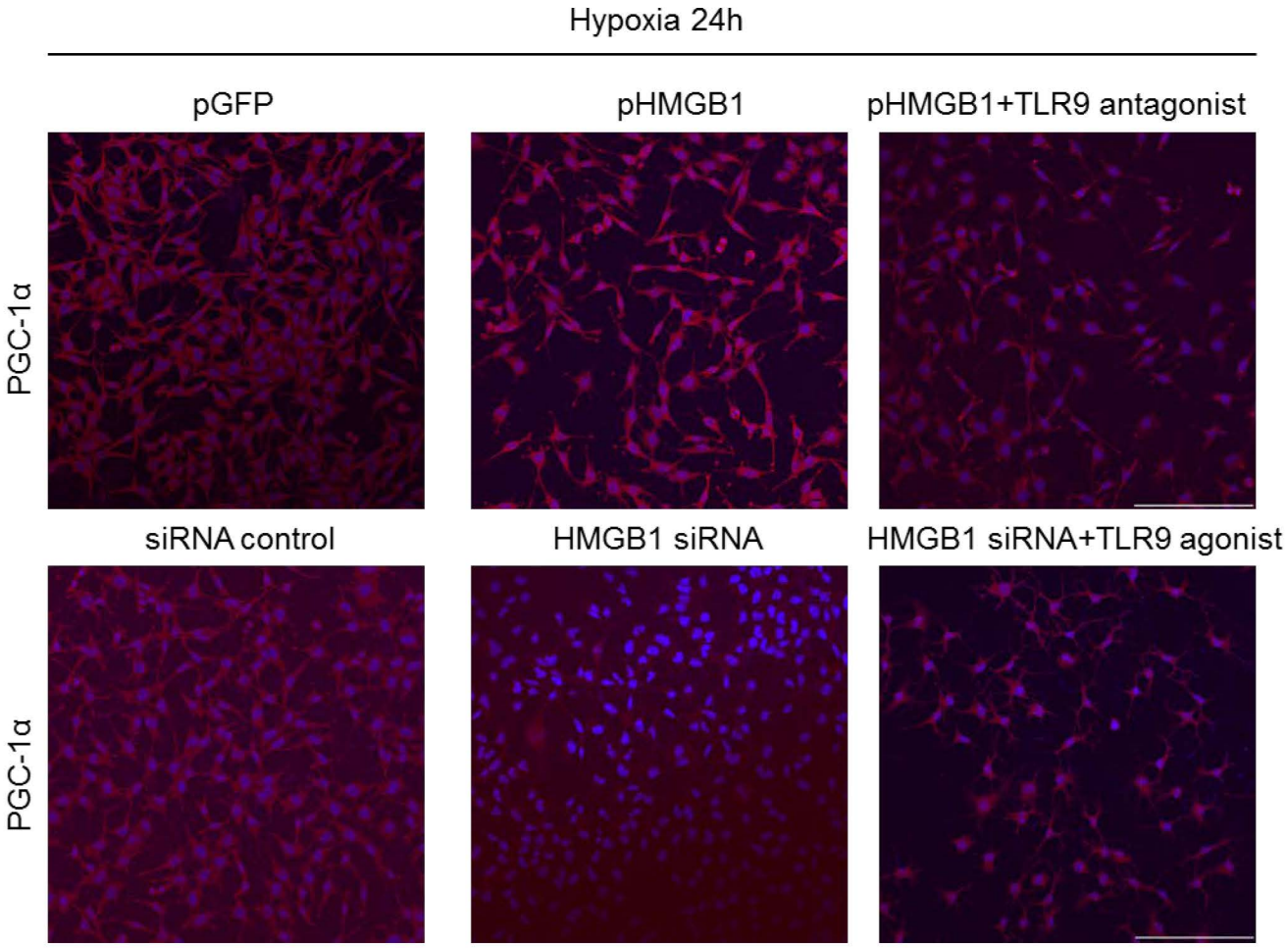

B